P-07-204

Oskarshamn site investigation

Rock matrix permeability measurements on core samples from borehole KLX03

Peter Vilks, Atomic Energy of Canada Ltd

December 2007

Svensk Kärnbränslehantering AB
Swedish Nuclear Fuel
and Waste Management Co
Box 250, SE-101 24 Stockholm
Tel +46 8 459 84 00

ISSN 1651-4416
SKB P-07-204

Oskarshamn site investigation

Rock matrix permeability measurements on core samples from borehole KLX03

Peter Vilks, Atomic Energy of Canada Ltd

December 2007

Keywords: Matrix permeability, Granite, Oskarshamn, AP PS 400-06-131.

Abstract

This report presents the results of matrix permeability measurements performed on rock samples taken from core hole KLX03 drilled at the Oskarshamn site investigation area. Permeability measurements were made at AECL's Whiteshell Laboratories using a range of confining pressures to simulate in-situ burial conditions. Measured permeability values in fracture free samples ranged from 4×10^{-23} to 6×10^{-19} m^2, corresponding to hydraulic conductivity values of 3×10^{-16} to 6×10^{-12} m/s. The presence of a fracture in one sample increased the permeability to 1×10^{-17} m^2. Increasing the confining pressure from 2 MPa to 15 MPa resulted in a reduction of measured permeability that ranged from a factor 4 to 154. Permeability measured normal to the core axis was a factor 3.9 to 19 lower than measured parallel to the core axis. The increase in measured permeability with sample depth suggests that samples were altered during drilling.

Sammanfattning

Denna rapport presenterar resultaten från mätningar av matrispermeabilitet utförda på borrkärneprover tagna från kärnborrhål KLX03 i Oskarshamns undersökningsområde. Permeabilitetsmätningar utfördes på AECL's Whiteshell Laboratories genom att trycksätta kärnproverna med olika yttre tryck i syfte att simulera tryckförhållandena in-situ. Uppmätta permeabilitetsvärden varierade från 4×10^{-23} till 6×10^{-19} m^2 för sprickfria prover, motsvarande en hydraulisk konduktivitet från 3×10^{-16} till 6×10^{-12} m/s. En av proverna inkluderade en mikrospricka, vilket ökade permeabiliteten till 1×10^{-17} m^2 för detta prov. Ökning av det yttre trycket från 2 MPa till 15 MPa resulterade i en minskning av den uppmätta permeabiliteten med en faktor 4 till 154. Permeabilitetsmätningar utförda vinkelrätt mot kärnaxeln var en faktor 4 till 19 lägre än mätningar längs kärnaxeln. Ökning av uppmätt permeabilitet mot djupet indikerar påverkan från borrningen.

Contents

1 Introduction

This document reports the results of permeability measurements performed at Whiteshell Laboratories using the High Pressure Radioisotope Migration (HPRM) apparatus /Vilks et al. 2004/. The work was carried out in accordance with activity plan AP PS 400-06-131. In Table 1-1 the controlling documents for performing this activity are listed. The activity plan is an SKB's internal controlling document.

This activity consisted of determining the rock matrix permeability of core samples from borehole KLX03, see Figure 1-1. The purpose is to get data on intact rock to be included in the safety assessment of the site.

Table 1-1. Controlling documents for performance of the activity.

Activity plan	Number	Version
Determination of rock matrix permeability on core samples from KLX03	AP PS 400-06-131	1.0

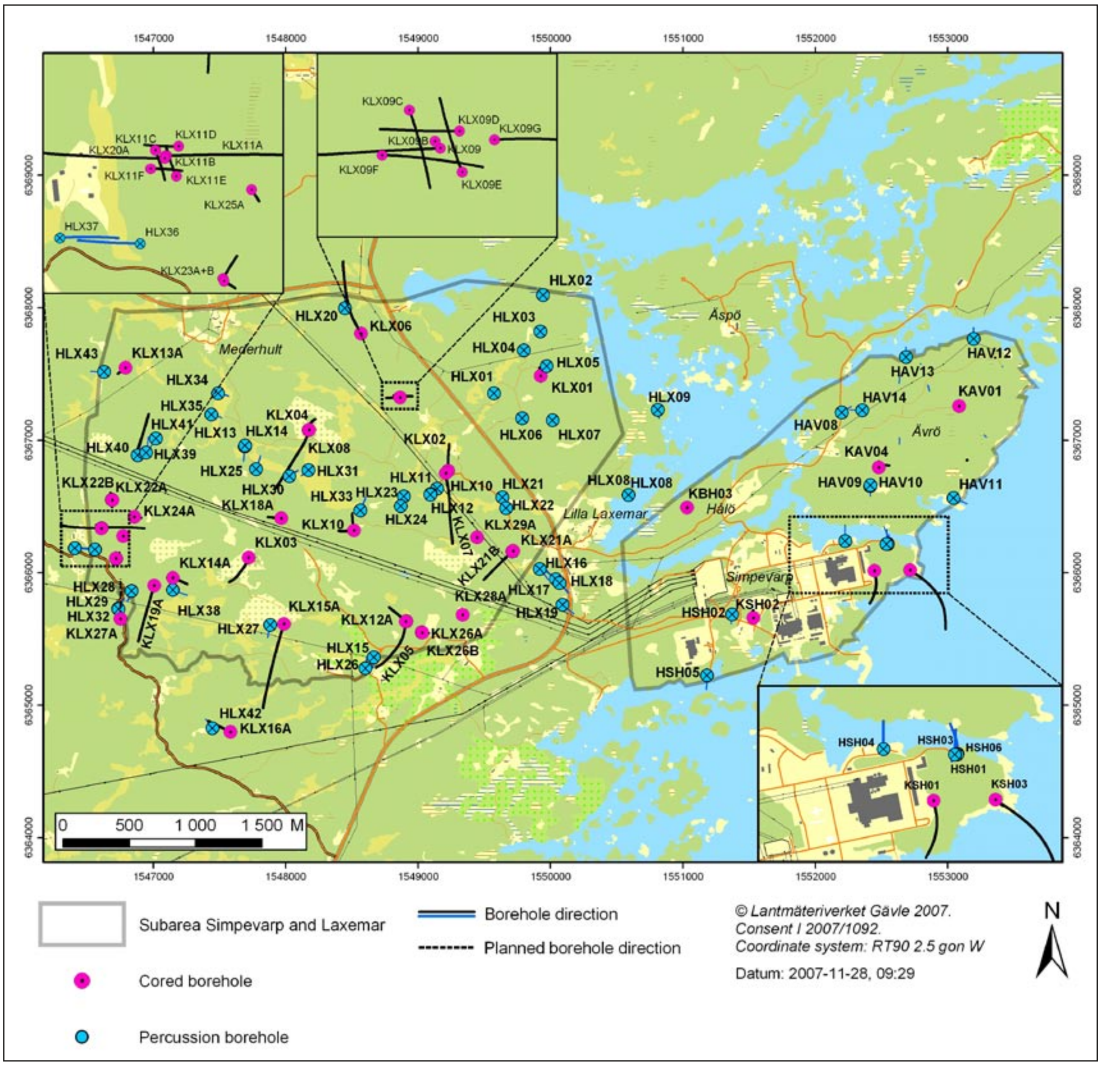

Figure 1-1. Map of the investigation area showing borehole locations.

2 Objective and scope

The objective of the work is to obtain data on the matrix permeability of rock formations at the Oskarshamn site. Matrix permeability is a measure of the ability of the rock's unfractured matrix to conduct water under a hydraulic gradient. The work scope consisted of measuring permeabilities of 6 core samples delivered to AECL by SKB. Permeabilities were determined by at least four confining pressures to evaluate the effects of sample alteration during drilling and to simulate the effect of lithostatic load. In selected samples permeability values were determined in two directions.

3 Equipment

3.1 Description of equipment/interpretation tools

Permeabilities of core samples are estimated at various confining pressures using the HPRM apparatus, described by /Drew and Vandergraaf 1989/. The HPRM consists of a core holder assembly, which is placed in a pressure vessel that can be operated with a maximum pressure of about 17 MPa. Core samples, with lengths of 0.5 to 2.0 cm, are placed between two stainless steel cylinders (Figure 3-1), each containing a centre drilled hole. The core samples and stainless steel cylinders are coated with a pliable RTV 108 silicon rubber adhesive (Figure 3-2) to isolate the core from the water used as the pressure medium in the pressure vessel. Once the core and stainless steel cylinders are connected to the lines used to pass sample fluid through the core, the pressure vessel is assembled and partially filled with water. A confining pressure is applied to the pressure vessel, which subjects the core sample to a tri-axial pressure along its length and both ends. Water is then pumped through the core at a constant flow rate and the pressure differential between the inlet and outlet side of the core is measured. Provided that the inlet pressure is not allowed to exceed the confining pressure, water flow is always from one end of the core to the other end, following the interconnected pore spacings. Once a steady water flow through the sample is established, the flow rate is determined by measuring the mass of water collected at the outlet over a given time interval. The entire HPRM facility is illustrated in (Figure 3-3).

Rock samples used for permeability estimation have a 25 mm diameter. These can be drilled from selected core samples using an orientation that is either parallel or perpendicular to the bedding planes.

Figure 3-1. *Rock core sample enclosed by end pieces to be used in a permeability measurement.*

Figure 3-2. *Rock core sample coated with silicon and ready to be loaded in pressure vessel for permeability measurement.*

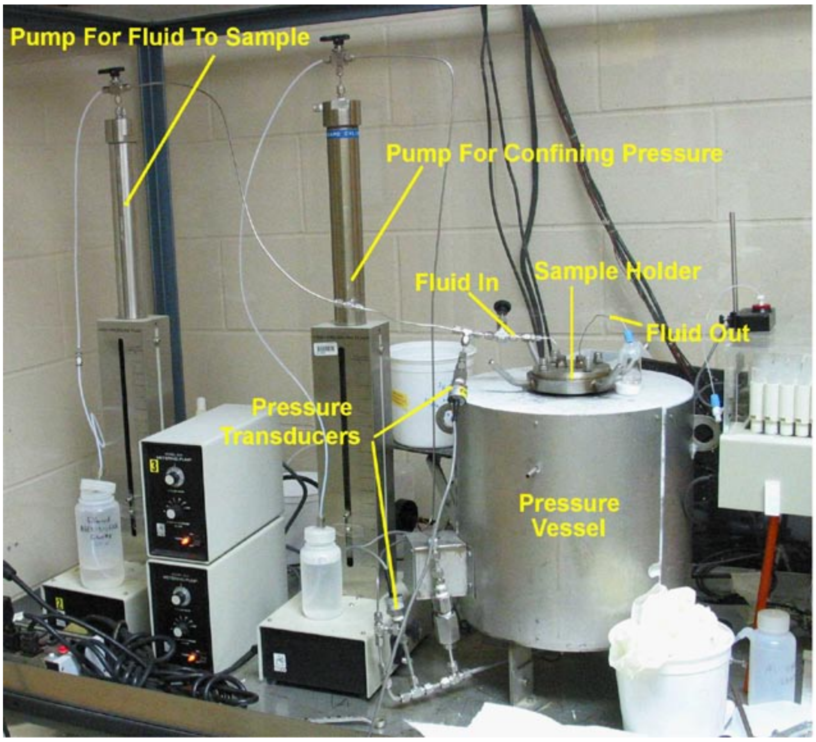

Figure 3-3. *HPRM facility for measuring permeability.*

The permeability of the core is given by

$$k = \frac{QL\mu}{A\Delta P} \tag{1}$$

where

k	is the permeability in m^2,
Q	is the volumetric flow rate in m^3/s,
L	is the length of the core in m,
μ	is the viscosity of the transport solution in $N \cdot s/m^2$,
A	is the cross sectional area of the core in m^2, and
ΔP	is the pressure differential between the inlet and outlet of the core in N/m^2.

In addition to sample dimensions, the parameters measured to calculate permeability consist of:

- The volumetric flow rate, Q, which is determined by collecting water for a measured time period. The volume of collected water is determined gravimetrically using a balance that is checked with weights that have their mass traceable to an ASTM Class 1 calibrated weight set.
- Pressure drop across sample, ΔP, is determined by a pressure transducer measuring the pressure of water being applied to one end of the sample. The pressure transducer is calibrated with a deadweight tester on a regular basis.

The error associated with a permeability measurement is the sum of errors from (1) the area of the sample cross section, (2) the sample length, (3) the pressure drop across the sample, and (4) the measured flow rate. The error attributed to the area of the cross section is about 1.6 percent. The error associated with sample length depends upon the total sample length, and varies between 4 and 5 percent for the samples used in this study. The error attributed to the pressure drop across the sample also depends on the magnitude of the pressure drop, typically varying between 1 and 20 percent. The error associated with the flow rate measurement is influenced by the total measured mass of fluid, as well as the time used to collect a given volume of fluid. Errors associated with flow rate measurements varied from 0.4 to 20 percent.

3.2 Rock samples

The rock samples were received from Eva Gustavsson (Deputy Activity Manager, SKB) on November 29, 2006. Table 3-1 summarizes the samples sent to AECL, as well as their locations in borehole KLX03. Figure 3-4 documents the core samples received from SKB, showing the variation in rock textures.

Table 3-1. List of rock samples from KLX03 for permeability measurements.

Core sample	Borehole length (m)*	Rock type
KLX03-5	355.66	Ävrö granite
KLX03-8	524.63	Ävrö granite
KLX03-9	590.12	Ävrö granite
KLX03-12	803.21	Quartz monzodiorite
KLX03-14	894.53	Quartz monzodiorite
KLX03-16	979.78	Quartz monzodiorite

Figure 3-4. *KLX03 core samples received from SKB.*

4 Execution

4.1 Sample preparation

The rock samples were cored with a water cooled diamond drill (Figure 4-1) to produce core samples with a 25 mm diameter. Every rock sample had one sample core drilled parallel to the core axis (Figure 4-2). Two rock samples were also drilled normal to the core axis to test the effect of sample orientation on permeability. Table 4-1 lists the samples cut for permeability measurements. The sample cores were cut into 5 to 16.5 mm thick slices to be used for the actual permeability measurements. After initial testing with thick samples, the sample thickness was reduced to 5 mm because the matrix permeability was found to be very low and sample thickness' greater than 5 mm would have resulted in excessively long measurement times.

Table 4-1. List of rock samples cored for permeability measurements.

Sample ID	From core sample	Comment
LAX-1	KLX03-5	Cut **parallel** to core axis
LAX-2	KLX03-9	Cut **parallel** to core axis
LAX-3	KLX03-9	Cut **normal** to core axis
LAX-4	KLX03-8	Cut **parallel** to core axis
LAX-5	KLX03-12	Cut **parallel** to core axis
LAX-6	KLX03-14	Cut **parallel** to core axis
LAX-7	KLX03-14	Cut **normal** to core axis
LAX-8	KLX03-16	Cut **parallel** to core axis

Figure 4-1. *Core samples cut for permeability measurements.*

Figure 4-2. Sample core cut parallel and normal to core axis. The core slices used for permeability measurements had a 25 mm diameter.

4.2 Permeability measurements

After the rock samples were placed between two end fittings, coated with silicon and placed into the pressure vessel, the confining pressure was initially increased to between 1.0 and 4.3 MPa. Once it was confirmed that the silicon coating isolating the sample from the confining high pressure fluid did not leak, distilled water was pumped into one end of the sample core using hydraulic pressures ranging from 0.2 to 6.5 MPa. Permeability measurements could begin once a steady flow of water was observed across the sample core. In some cases the time to reach a steady flow was up to one or two weeks. The flow rate was determined by gravimetrically measuring the amount of water collected over time periods ranging from 1 hour to several days. Once several permeability measurements were performed at a given confining pressure, the confining pressure was increased up to values as high as 16.4 MPa to produce permeability measurements over a range of confining pressures.

4.3 Data handling/post processing

The raw data was recorded on data sheets stored in a binder dedicated to the HPRM. The raw data was transferred to an Excel spreadsheet to calculate permeability, conductivity and associated error using Equation 1.

4.4 Nonconformities

The sample core KLX03-8 appeared to contain a fracture running along its length. Therefore, sample KLX03-9 was used to cut samples LAX-2 and LAX-3, instead of using KLX03-8 as laid out in the activity plan. Table 4-1 identifies the samples used for permeability measurements as used in this study. Sample LAX-5 also contained a fracture and was expected to have a higher permeability.

5 Results

The results of permeability measurements of rock samples from core KLX03 are tabulated in Table 5-1. The results for each core sample are given in the order of measurement. The data for each measurement include the confining pressure, the pressure drop across the sample and the observed flow rate. Using the measured pressure drop and flow rate, and the sample length and surface area, the permeability was calculated using Equation 1. The table also includes values of hydraulic conductivity (m/s) corresponding to the calculated permeability values (m^2). The reported error values were estimated for each measurement.

The effect of confining pressure on permeability measurements is illustrated in Figure 5-1. Note that sample LAX-1 was not included in this figure because the confining pressure for this sample did not go beyond 7 MPa. When the confining pressure was increased from 2 MPa to 15 MPa most samples displayed reductions in permeability that ranged from a factor 4 to 154. This suggests that rock samples may have been altered by stress relief during drilling. With the application of a high confining pressure a portion of the additional porosity created by sample alteration was closed to flow.

Assuming that permeability values measured at high confining pressures are more representative of in-situ conditions, average permeability values obtained at confining pressures above 14 MPa are given in Table 5-2. Note that sample LAX-1 is an exception because permeability values at high confining pressure were not available for this sample. The average permeability values in Table 5-2 are plotted versus sample depth in Figure 5-2. The estimated permeabilities increase with sample depth, possibly because with increasing depth and confining pressure there is more sample alteration during drilling. The permeability values measured parallel to the core axis were higher than permeabilities measured normal to the core axis by factors of 3.9 (LAX-2 and LAX-3) and 19 (LAX-6 and LAX-7). This suggests that matrix permeability may not be isotropic, with the anisotropy increasing with sample depth.

Table 5-1. Permeability results KLX03.

Sample	Confining pressure (MPa)	Pressure drop (MPa)	Flow rate (m^3/s)	Permeability (m^2)	Conductivity (m/s)
LAX-1 (355.66 m)	1.70	1.00	8.3×10^{-16}	$(3.1\pm2.3)\times10^{-23}$	$(2.7\pm2.0)\times10^{-16}$
Parallel to Core Axis	2.00	0.55	1.1×10^{-16}	$(7.2\pm0.2)\times10^{-24}$	$(6.3\pm0.1)\times10^{-17}$
diameter: 25 mm	2.20	1.65	1.5×10^{-15}	$(3.3\pm1.5)\times10^{-23}$	$(2.9\pm1.3)\times10^{-16}$
area: 491 mm^2	7.00	5.00	1.5×10^{-15}	$(1.1\pm0.4)\times10^{-23}$	$(9.7\pm3.1)\times10^{-17}$
length: 16.5 mm	6.60	5.80	1.7×10^{-14}	$(1.1\pm0.2)\times10^{-22}$	$(9.8\pm1.7)\times10^{-16}$
LAX-2 (590.12 m)	4.3	2.9	2.0×10^{-13}	$(1.5\pm0.1)\times10^{-21}$	$(1.3\pm0.1)\times10^{-14}$
Parallel to Core Axis	5.2	4.1	4.1×10^{-13}	$(2.2\pm0.1)\times10^{-21}$	$(1.9\pm0.1)\times10^{-14}$
diameter: 25 mm	8.1	4.9	3.5×10^{-12}	$(1.6\pm0.2)\times10^{-20}$	$(1.4\pm0.2)\times10^{-13}$
area: 491 mm^2	8.3	5.0	2.9×10^{-13}	$(1.3\pm0.1)\times10^{-21}$	$(1.1\pm0.1)\times10^{-14}$
length: 9.7 mm	8.5	5.0	4.0×10^{-13}	$(1.8\pm0.3)\times10^{-21}$	$(1.5\pm0.2)\times10^{-14}$
	6.3	5.4	5.8×10^{-13}	$(2.4\pm0.3)\times10^{-21}$	$(2.1\pm0.2)\times10^{-14}$
	8.4	5.5	4.0×10^{-13}	$(1.6\pm0.2)\times10^{-21}$	$(1.4\pm0.2)\times10^{-14}$
	9.1	5.7	2.5×10^{-13}	$(9.8\pm0.6)\times10^{-22}$	$(8.5\pm0.5)\times10^{-15}$
	11.0	6.1	3.3×10^{-13}	$(1.2\pm0.1)\times10^{-21}$	$(1.1\pm0.1)\times10^{-14}$
	11.8	6.2	2.6×10^{-13}	$(9.3\pm2.1)\times10^{-22}$	$(8.1\pm1.8)\times10^{-15}$
	12.0	6.5	1.4×10^{-13}	$(4.6\pm1.5)\times10^{-22}$	$(4.1\pm1.3)\times10^{-15}$
	11.9	6.5	2.0×10^{-13}	$(7.0\pm1.2)\times10^{-22}$	$(6.1\pm1.0)\times10^{-15}$
	11.7	6.4	9.2×10^{-14}	$(3.2\pm0.7)\times10^{-22}$	$(2.8\pm0.6)\times10^{-15}$
	11.6	6.2	3.0×10^{-13}	$(1.1\pm0.1)\times10^{-21}$	$(9.4\pm0.6)\times10^{-15}$
	15.2	6.1	2.5×10^{-13}	$(9.2\pm1.5)\times10^{-22}$	$(8.0\pm1.3)\times10^{-15}$
	15.1	5.8	2.1×10^{-13}	$(7.9\pm0.4)\times10^{-22}$	$(6.9\pm0.4)\times10^{-15}$
LAX-3 (590.12 m)	1.9	0.4	1.9×10^{-13}	$(6.2\pm1.3)\times10^{-21}$	$(5.4\pm1.1)\times10^{-14}$
Normal to Core Axis	1.7	0.7	3.2×10^{-13}	$(5.2\pm1.0)\times10^{-21}$	$(4.6\pm0.8)\times10^{-14}$
diameter: 25 mm	2.6	0.8	2.3×10^{-13}	$(3.3\pm0.4)\times10^{-21}$	$(2.9\pm0.4)\times10^{-14}$
area: 491 mm^2	3.5	0.9	5.9×10^{-14}	$(7.5\pm2.4)\times10^{-22}$	$(6.5\pm2.1)\times10^{-15}$
length: 5.0 mm	7.1	1.5	6.3×10^{-14}	$(5.0\pm0.7)\times10^{-22}$	$(4.4\pm0.6)\times10^{-15}$
	8.1	2.3	3.0×10^{-13}	$(1.5\pm0.4)\times10^{-21}$	$(1.3\pm0.3)\times10^{-14}$
	8.3	2.6	1.9×10^{-13}	$(8.5\pm4.4)\times10^{-22}$	$(7.4\pm3.9)\times10^{-15}$
	7.9	2.8	2.9×10^{-13}	$(1.2\pm0.2)\times10^{-21}$	$(1.0\pm0.2)\times10^{-14}$
	11.3	3.0	1.5×10^{-13}	$(5.7\pm1.6)\times10^{-22}$	$(4.9\pm1.4)\times10^{-15}$
	14.2	3.0	7.1×10^{-14}	$(2.7\pm2.1)\times10^{-22}$	$(2.4\pm1.8)\times10^{-15}$
	13.6	3.0	1.8×10^{-13}	$(7.0\pm0.7)\times10^{-22}$	$(6.1\pm0.6)\times10^{-15}$
	15.4	2.9	4.4×10^{-14}	$(1.7\pm0.8)\times10^{-22}$	$(1.5\pm0.7)\times10^{-15}$

Table 5-1. Permeability results KLX03…continued.

Sample	Confining pressure (MPa)	Pressure drop (MPa)	Flow rate (m^3/s)	Permeability (m^2)	Conductivity (m/s)
LAX-4 (524.63 m)	2.4	0.8	1.4×10^{-12}	$(2.2\pm0.4)\times10^{-20}$	$(1.9\pm0.3)\times10^{-13}$
Parallel to Core Axis	2.3	0.7	1.3×10^{-12}	$(2.1\pm0.4)\times10^{-20}$	$(1.8\pm0.3)\times10^{-13}$
diameter: 25 mm	5.0	0.8	1.4×10^{-12}	$(2.1\pm0.3)\times10^{-20}$	$(1.8\pm0.3)\times10^{-13}$
area: 491 mm^2	5.0	1.0	1.6×10^{-12}	$(1.9\pm0.3)\times10^{-20}$	$(1.7\pm0.3)\times10^{-13}$
length: 5.0 mm	5.6	1.3	2.9×10^{-12}	$(2.7\pm0.3)\times10^{-20}$	$(2.4\pm0.2)\times10^{-13}$
	6.1	1.5	4.7×10^{-12}	$(3.6\pm0.4)\times10^{-20}$	$(3.1\pm0.4)\times10^{-13}$
	10.0	1.7	4.1×10^{-12}	$(2.8\pm0.3)\times10^{-20}$	$(2.4\pm0.3)\times10^{-13}$
	10.1	1.8	4.1×10^{-12}	$(2.6\pm0.3)\times10^{-20}$	$(2.3\pm0.3)\times10^{-13}$
	13.9	1.9	4.3×10^{-12}	$(2.7\pm0.4)\times10^{-20}$	$(2.3\pm0.4)\times10^{-13}$
	13.7	2.0	3.4×10^{-12}	$(2.0\pm0.2)\times10^{-20}$	$(1.7\pm0.2)\times10^{-13}$
	13.5	1.0	9.4×10^{-13}	$(1.1\pm0.1)\times10^{-20}$	$(9.4\pm1.0)\times10^{-14}$
	14.8	0.2	5.6×10^{-14}	$(4.2\pm2.9)\times10^{-21}$	$(3.7\pm2.5)\times10^{-14}$
	14.7	1.5	3.9×10^{-13}	$(3.0\pm5.8)\times10^{-21}$	$(2.6\pm0.5)\times10^{-14}$
	14.2	2.7	8.5×10^{-13}	$(3.6\pm2.8)\times10^{-21}$	$(3.1\pm0.3)\times10^{-14}$
	14.6	3.7	1.8×10^{-12}	$(5.5\pm4.0)\times10^{-21}$	$(4.8\pm0.4)\times10^{-14}$
LAX-5 (803.21 m)	2.0	0.6	3.9×10^{-9}	$(8.1\pm1.9)\times10^{-17}$	$(7.0\pm1.7)\times10^{-10}$
Parallel to Core Axis	4.2	0.5	3.9×10^{-9}	$(9.9\pm2.4)\times10^{-17}$	$(8.6\pm2.1)\times10^{-10}$
diameter: 25 mm	8.2	1.0	2.8×10^{-9}	$(3.4\pm0.6)\times10^{-17}$	$(3.0\pm0.6)\times10^{-10}$
area: 491 mm^2	12.2	1.3	2.0×10^{-9}	$(1.8\pm0.3)\times10^{-17}$	$(1.6\pm0.3)\times10^{-10}$
length: 5.0 mm	15.0	1.6	2.0×10^{-9}	$(1.5\pm0.2)\times10^{-17}$	$(1.3\pm0.2)\times10^{-10}$
LAX-6 (894.53 m)	1.5	0.4	1.7×10^{-12}	$(5.6\pm1.1)\times10^{-20}$	$(4.9\pm1.0)\times10^{-13}$
Parallel to Core Axis	2.6	0.7	4.4×10^{-12}	$(7.8\pm1.1)\times10^{-20}$	$(6.8\pm0.9)\times10^{-13}$
diameter: 25 mm	3.2	0.4	3.4×10^{-12}	$(9.6\pm1.9)\times10^{-20}$	$(8.4\pm1.6)\times10^{-13}$
area: 491 mm^2	3.1	0.2	2.3×10^{-12}	$(1.3\pm0.4)\times10^{-19}$	$(1.1\pm0.4)\times10^{-12}$
length: 5.0 mm	7.6	0.4	1.7×10^{-12}	$(4.9\pm0.9)\times10^{-20}$	$(4.2\pm0.8)\times10^{-13}$
	8.1	0.4	1.7×10^{-12}	$(4.8\pm0.9)\times10^{-20}$	$(4.1\pm0.8)\times10^{-13}$
	8.1	0.7	2.6×10^{-12}	$(4.3\pm0.7)\times10^{-20}$	$(3.8\pm0.6)\times10^{-13}$
	8.6	1.0	3.0×10^{-12}	$(3.4\pm0.4)\times10^{-20}$	$(3.0\pm0.3)\times10^{-13}$
	9.2	1.4	4.4×10^{-12}	$(3.6\pm0.4)\times10^{-20}$	$(3.1\pm0.4)\times10^{-13}$
	9.4	1.5	4.5×10^{-12}	$(3.4\pm0.4)\times10^{-20}$	$(3.0\pm0.4)\times10^{-13}$
	14.6	1.4	2.8×10^{-12}	$(2.3\pm0.2)\times10^{-20}$	$(2.0\pm0.2)\times10^{-13}$
	15.2	0.7	1.5×10^{-12}	$(2.7\pm0.4)\times10^{-20}$	$(2.4\pm0.3)\times10^{-13}$
	14.7	0.9	1.0×10^{-12}	$(1.3\pm0.2)\times10^{-20}$	$(1.1\pm0.1)\times10^{-13}$
	13.2	3.2	1.2×10^{-12}	$(4.4\pm0.3)\times10^{-21}$	$(3.8\pm0.3)\times10^{-14}$
	14.6	5.5	3.6×10^{-12}	$(7.4\pm0.8)\times10^{-21}$	$(6.5\pm0.7)\times10^{-14}$
	15.0	5.7	3.0×10^{-12}	$(6.0\pm0.7)\times10^{-21}$	$(5.2\pm0.6)\times10^{-14}$
	15.2	5.9	3.3×10^{-12}	$(6.5\pm0.5)\times10^{-21}$	$(5.6\pm0.5)\times10^{-14}$

Table 5-1. Permeability results KLX03…continued.

Sample	Confining pressure (MPa)	Pressure drop (MPa)	Flow rate (m^3/s)	Permeability (m^2)	Conductivity (m/s)
LAX-7 (895.53 m)	2.3	0.9	2.3×10^{-12}	$(2.8\pm0.4)\times10^{-20}$	$(2.5\pm0.3)\times10^{-13}$
Normal to Core Axis	1.7	0.7	2.5×10^{-12}	$(3.7\pm0.6)\times10^{-20}$	$(3.2\pm0.5)\times10^{-13}$
diameter: 25 mm	5.0	0.9	3.3×10^{-12}	$(3.7\pm0.5)\times10^{-20}$	$(3.2\pm0.5)\times10^{-13}$
area: 491 mm^2	4.5	0.8	2.3×10^{-12}	$(2.8\pm0.4)\times10^{-20}$	$(2.5\pm0.3)\times10^{-13}$
length: 4.5 mm	7.0	0.9	2.3×10^{-12}	$(2.6\pm0.4)\times10^{-20}$	$(2.3\pm0.3)\times10^{-13}$
	7.0	1.3	1.9×10^{-12}	$(1.5\pm0.2)\times10^{-20}$	$(1.3\pm0.2)\times10^{-13}$
	9.1	1.5	2.1×10^{-12}	$(1.4\pm0.2)\times10^{-20}$	$(1.2\pm0.1)\times10^{-13}$
	12.3	0.9	6.4×10^{-13}	$(7.3\pm0.9)\times10^{-21}$	$(6.4\pm0.8)\times10^{-14}$
	12.4	1.1	2.0×10^{-13}	$(1.9\pm0.4)\times10^{-21}$	$(1.6\pm0.3)\times10^{-14}$
	14.7	0.9	7.1×10^{-14}	$(7.9\pm2.7)\times10^{-22}$	$(6.9\pm2.4)\times10^{-15}$
	15.3	1.8	1.9×10^{-13}	$(1.1\pm0.1)\times10^{-21}$	$(9.3\pm1.0)\times10^{-15}$
	16.0	2.6	2.0×10^{-13}	$(7.8\pm1.1)\times10^{-22}$	$(6.8\pm1.0)\times10^{-15}$
	16.4	2.7	6.2×10^{-14}	$(2.4\pm2.6)\times10^{-22}$	$(2.1\pm2.3)\times10^{-15}$
LAX-8 (979.78 m)	1.0	0.2	4.5×10^{-12}	$(2.6\pm0.8)\times10^{-19}$	$(2.3\pm0.7)\times10^{-12}$
Parallel to Core Axis	1.0	0.2	1.1×10^{-11}	$(6.4\pm2.1)\times10^{-19}$	$(5.6\pm1.9)\times10^{-12}$
diameter: 25 mm	2.0	0.2	1.1×10^{-11}	$(6.4\pm2.2)\times10^{-19}$	$(5.6\pm1.9)\times10^{-12}$
area: 491 mm^2	4.1	0.2	1.0×10^{-11}	$(5.1\pm1.6)\times10^{-19}$	$(4.4\pm1.4)\times10^{-12}$
length: 5.0 mm	4.1	0.3	1.0×10^{-11}	$(4.2\pm1.3)\times10^{-19}$	$(3.6\pm1.1)\times10^{-12}$
	4.8	0.3	1.3×10^{-11}	$(5.9\pm1.5)\times10^{-19}$	$(5.1\pm1.3)\times10^{-12}$
	8.0	0.2	1.1×10^{-11}	$(6.1\pm2.0)\times10^{-19}$	$(5.3\pm1.8)\times10^{-12}$
	8.1	0.3	1.1×10^{-11}	$(5.0\pm1.4)\times10^{-19}$	$(4.3\pm1.2)\times10^{-12}$
	12.2	0.4	1.1×10^{-11}	$(3.5\pm0.8)\times10^{-19}$	$(3.0\pm0.7)\times10^{-12}$
	12.6	0.4	1.1×10^{-11}	$(3.1\pm0.6)\times10^{-19}$	$(2.7\pm0.5)\times10^{-12}$
	11.9	0.5	1.1×10^{-11}	$(2.6\pm0.4)\times10^{-19}$	$(2.2\pm0.4)\times10^{-12}$
	13.6	0.6	1.3×10^{-11}	$(2.5\pm0.4)\times10^{-19}$	$(2.2\pm0.3)\times10^{-12}$
	13.7	0.7	1.6×10^{-11}	$(2.6\pm0.4)\times10^{-19}$	$(2.3\pm0.3)\times10^{-12}$
	14.3	0.7	1.2×10^{-11}	$(2.1\pm0.3)\times10^{-19}$	$(1.8\pm0.3)\times10^{-12}$
	14.5	0.6	9.0×10^{-12}	$(1.7\pm0.3)\times10^{-19}$	$(1.5\pm0.2)\times10^{-12}$

Table 5-2. Average permeability and conductivity values for confining pressures greater than 14 MPa.

Sample	Permeability (m^2)	Conductivity (m/s)
LAX -1*	$(4\pm4)\times10^{-23}$	$(3\pm4)\times10^{-16}$
LAX-2	$(8.6\pm0.9)\times10^{-22}$	$(7.5\pm0.8)\times10^{-15}$
LAX-3	$(2.2\pm0.7)\times10^{-22}$	$(1.9\pm0.6)\times10^{-15}$
LAX-4	$(4.1\pm1.1)\times10^{-21}$	$(3.6\pm0.9)\times10^{-14}$
LAX-5	1.45×10^{-17}	1.27×10^{-10}
LAX-6	$(1.4\pm0.9)\times10^{-20}$	$(1.2\pm0.8)\times10^{-13}$
LAX-7	$(7.2\pm3.5)\times10^{-22}$	$(6.3\pm3.1)\times10^{-15}$
LAX-8	$(1.9\pm0.3)\times10^{-19}$	$(1.7\pm0.2)\times10^{-12}$

* Average for confining pressures from 1.7 to 7.0 MPa.

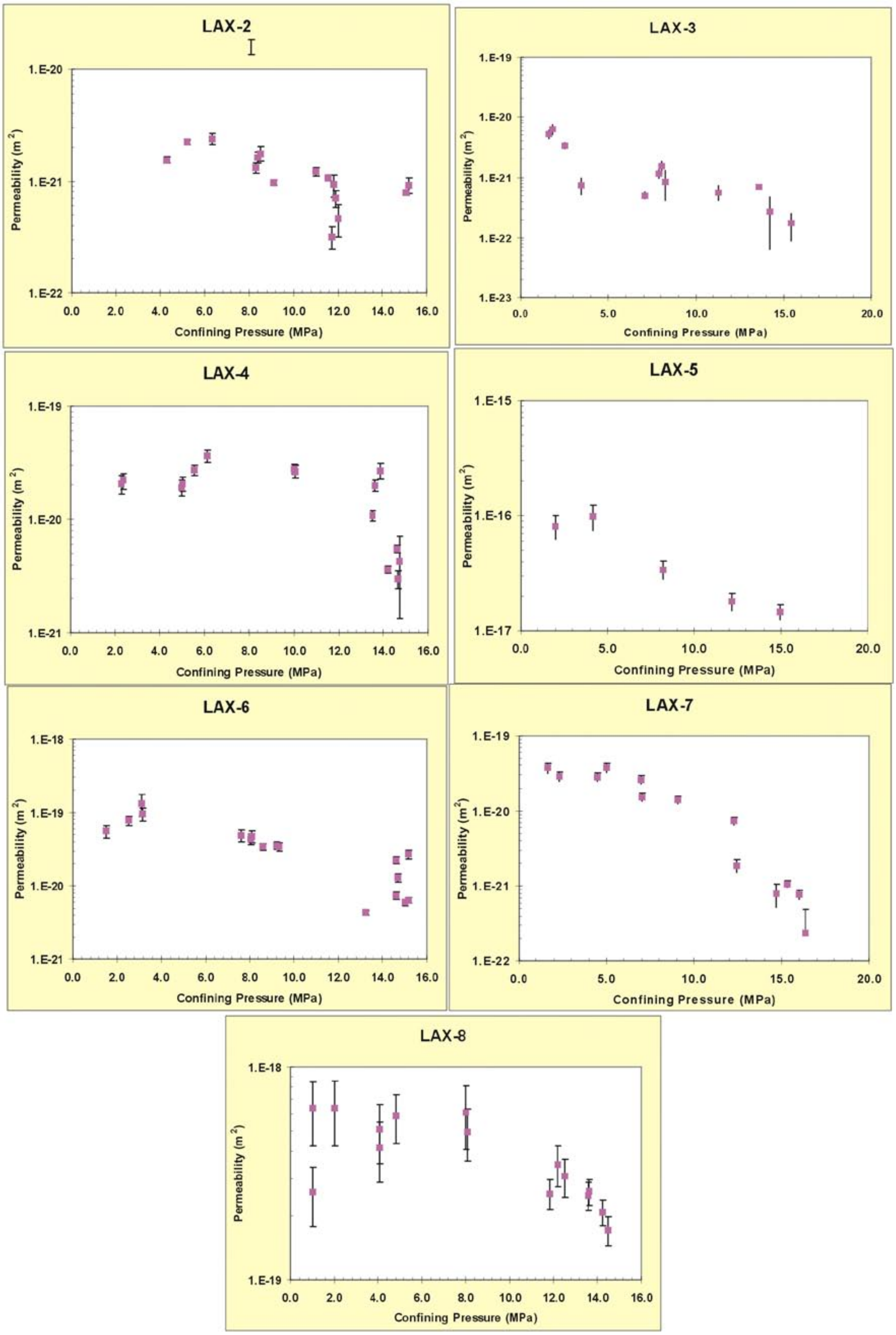

Figure 5-1. *Effect of confining pressure on permeability values.*

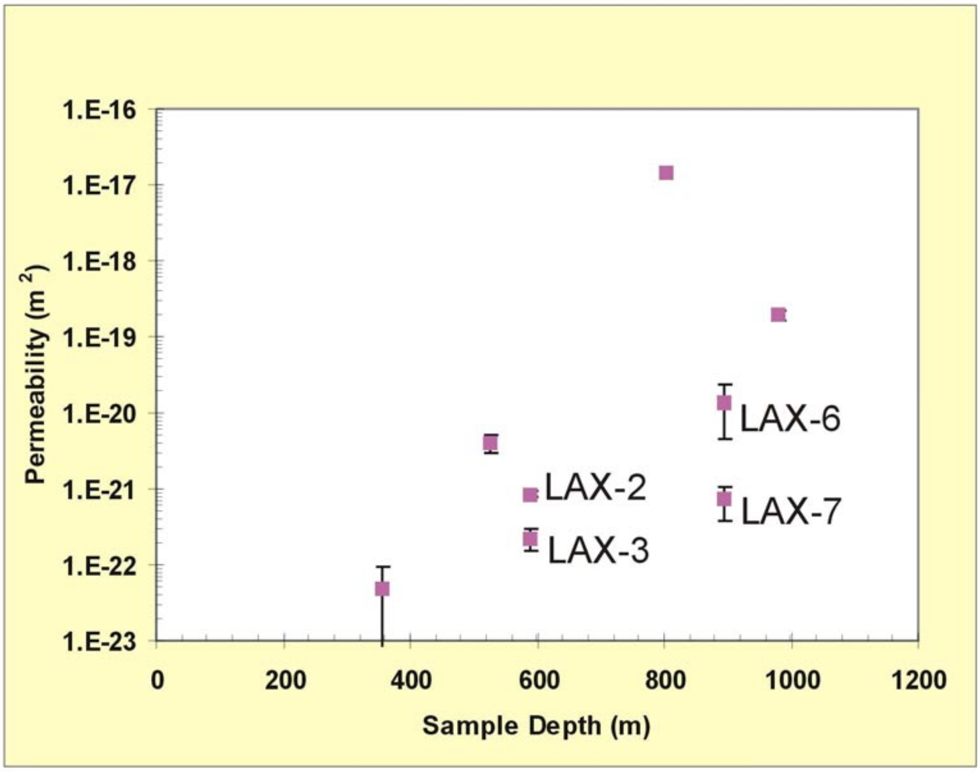

Figure 5-2. *Effect of sample depth on average permeability values.*

References

Drew D J, Vandergraaf T T, 1989. Construction and operation of a high-pressure radioisotope migration apparatus. Atomic Energy of Canada Limited Technical Record, TR-476.

Vilks P, Miller N H, Stanchell F W, 2004. Phase II in-situ diffusion experiment. AECL Report no: 06819-Rep-01200-10128-R00.